UCD School of Civil Engineering
University College Dublin

REPLY TO REVIEWERS

Manuscript No.:	wes-2026-70
Title:	Machine Learning Framework for Scour Detection Across Multiple Offshore Wind Farms
Authors:	Mahmoud Abdelhak; Luke J Prendergast; Jacques Tott-Buswell; Ramin Ghiasi; Abdollah Malekjafarian
Review for:	Wind Energy Science

NOTE TO REVIEWERS: We would like to express our gratitude to the Reviewers for the valuable remarks addressed in their reports regarding our manuscript, which helped us improve our work.

This letter serves as a guide to identifying all changes introduced into the reviewed version of the manuscript. It provides a point-by-point response to all pertinent remarks from the Reviewers. The changes in the manuscript are identified by blue text in the manuscript using the Track Changes tool in MS Word, in the file "Revised_Manuscript_with_Track_Changes".

Reviewer 1

Comment (1): Firstly, appropriate baselines are missing. Without these, some of the conclusions of the contribution can be called into question. Namely: The Domain-Adversarial NN (DANN) is only compared to Causal Disentanglement Domain Generalisation (CDDG), but there is no baseline present without Domain Generalisation. Therefore, we cannot extrapolate what is gained by this approach compared to simply training a classifier. This is especially relevant given the results for Tasks 2-4, where the scour detection appears to be highly training turbine-dependent and generalisation appears to be lacking. In this context, it is important to understand if there is any generalisation gain from adversarial training or if the results depend solely on the training data.

Reply to Comment (1): Thank you for this valuable comment. We agree that comparing the proposed domain generalisation (DG) Domain-Adversarial NN (DANN) framework only against Causal Disentanglement Domain Generalisation (CDDG) does not fully quantify the benefit provided by domain generalisation itself. To address this concern, an additional baseline corresponding to a conventional supervised classifier trained using the same source-domain data and network architecture is implemented, but without any domain generalisation mechanism, allowing the isolation between the DG contribution and the influence of the selected source turbine. The revised manuscript now presents the generalisation capability for scour detection at inter-farm level with and without the implementation of DG strategy by comparing the conventional classifier and DANN across all evaluation protocols. The results demonstrate that although the conventional classifier achieves satisfactory performance on the source domains, its performance deteriorates significantly when evaluated on previously unseen target turbines due to the substantial domain shift arising from differences in soil properties, water depth, structural characteristics, and environmental loading conditions. In contrast, DANN consistently achieves higher classification accuracy and improved robustness across the unseen target turbines by learning representations that are less sensitive to domain-specific characteristics while preserving scour-related information. This demonstrates that the observed improvement is not solely attributable to the selection of the source turbines, but also to the domain-invariant feature learning enabled by the adversarial training process. While these tasks remain inherently more challenging because of the increased discrepancy between the selected source and target turbines, the DG-based approaches still provide measurable improvements over the conventional classifier. This confirms that the degradation observed in these tasks primarily reflects the severity of the domain shift rather than the ineffectiveness of the DG framework. Consequently, the revised results more clearly distinguish the effect of source-domain selection from the benefit provided by domain generalisation.

A paragraph of text has been added to the revised manuscript, shown in blue text. For convenience, this is also shown below. (Relevant text from manuscript Section 4.1, lines 570-590)

To assess the benefit of applying DG strategies to generalise scour detection at inter-farm level, a conventional supervised learning baseline model developed using the empirical risk minimisation (ERM) method is also implemented. The ERM model employs the same network architecture, training data, and optimisation strategy as the proposed DANN framework, with the only difference being the absence of the domain-adversarial component. Consequently, the ERM model learns solely by minimising the classification loss on the source-domain data without enforcing domain-invariant feature representations. Comparing the ERM baseline with DANN enables assessing the performance improvement obtained due to applying DG, along with isolating it from the influence of the source turbines selection. Any performance difference between the ERM baseline and the DG approaches can be directly attributed to the ability of DG methods to learn feature representations that are robust to the distribution shifts between source and target turbines. The capability of the DANN-based scour detection method is further assessed to mitigate the domain shift arising from variations in soil properties, water depth, turbine structural characteristics, and environmental loading conditions across different OWFs. Figures A1-4 demonstrate the model performance for detecting scour using different training and testing tasks (Tasks 1-4) and are presented in the Appendix. The results show that low to moderate gains in performance are obtained due to the application of DG. For example, the application of DG leads to enhancement in scour detection at shallow water turbines (T1.1, T1.2, T2.1, T2.2, T3.1, and T3.2) across different wind farms, reaching 23% enhancement for detecting 6m scour at T3.1. Under Task 1 training, the application of DG shows the highest impact at detecting scour at farm 3. Similar improvement was obtained for training Tasks 3 and 4. However, in enhancing the detectability for shallow scour depths at deep turbine T6-T11 across different turbines at Task 2, its application induced an adverse effect at shallow water turbines. The observed improvement is not solely attributable to the selection of the source turbines, but also to the domain-invariant feature learning enabled by the adversarial training process.

A paragraph of text has been added to the revised manuscript, shown in blue text. For convenience, this is also shown below. (Relevant text from manuscript Section Appendix A , lines 859-870)

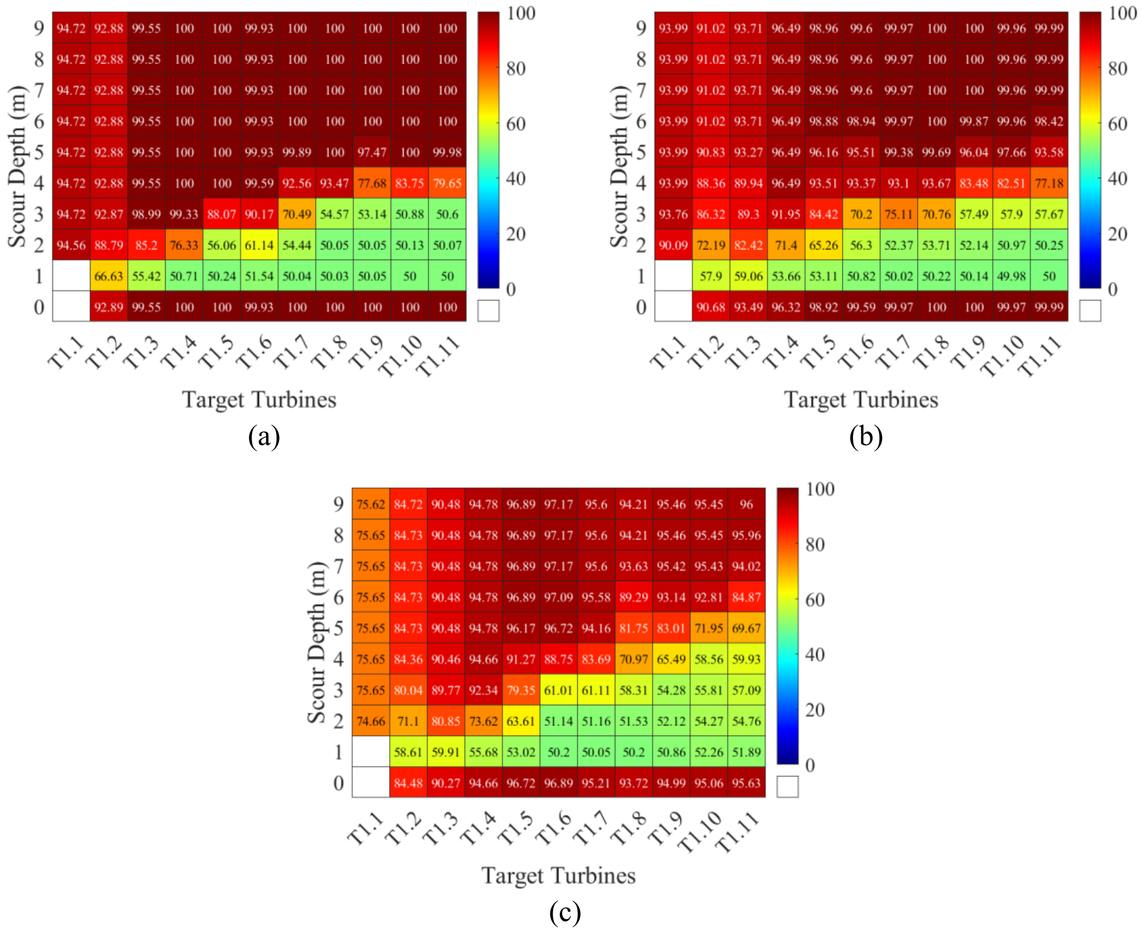

Figure A1: The baseline model performance when trained on Task 1 and evaluated on target OWTs located at a) Farm 1, b) Farm 2, and c) Farm 3.

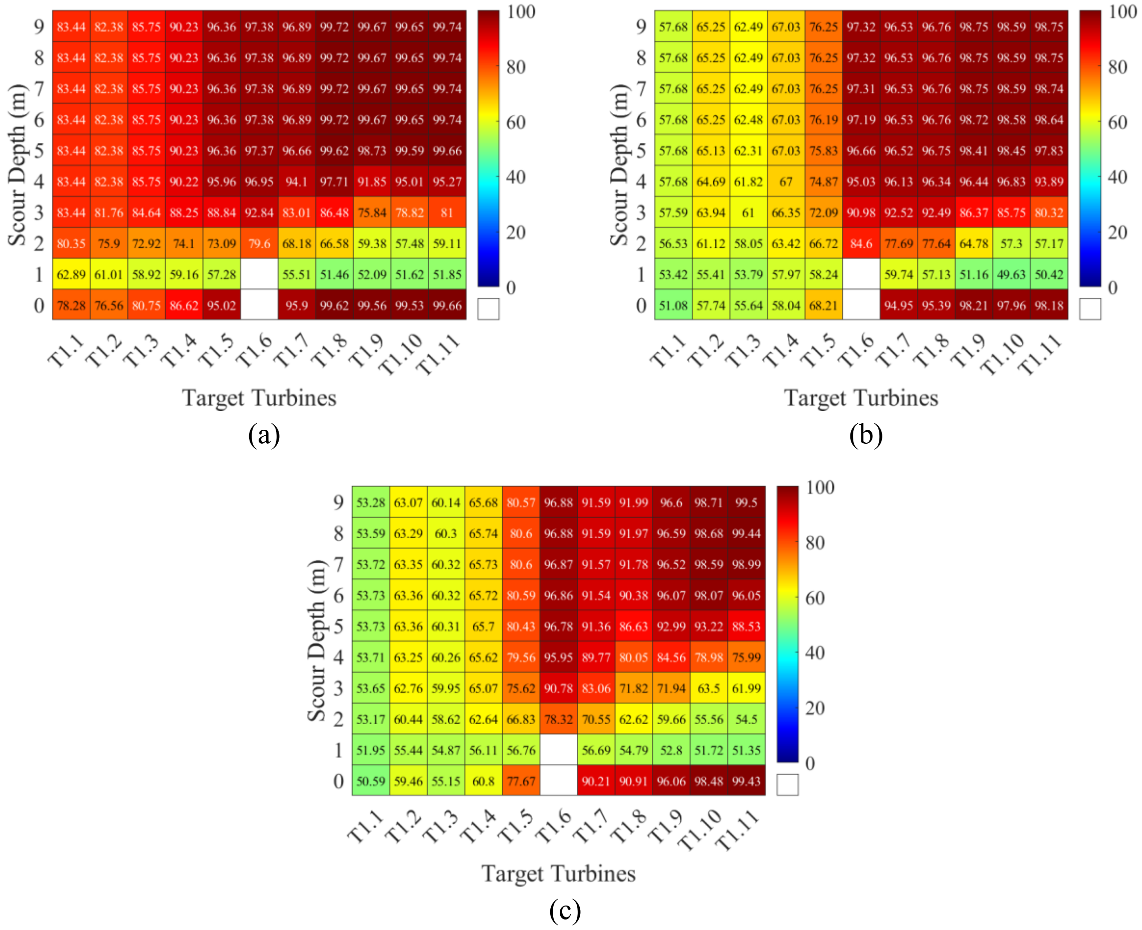

Figure A2: The baseline model performance when trained on Task 2 and evaluated on target OWTs located at a) Farm 1, b) Farm 2, and c) Farm 3.

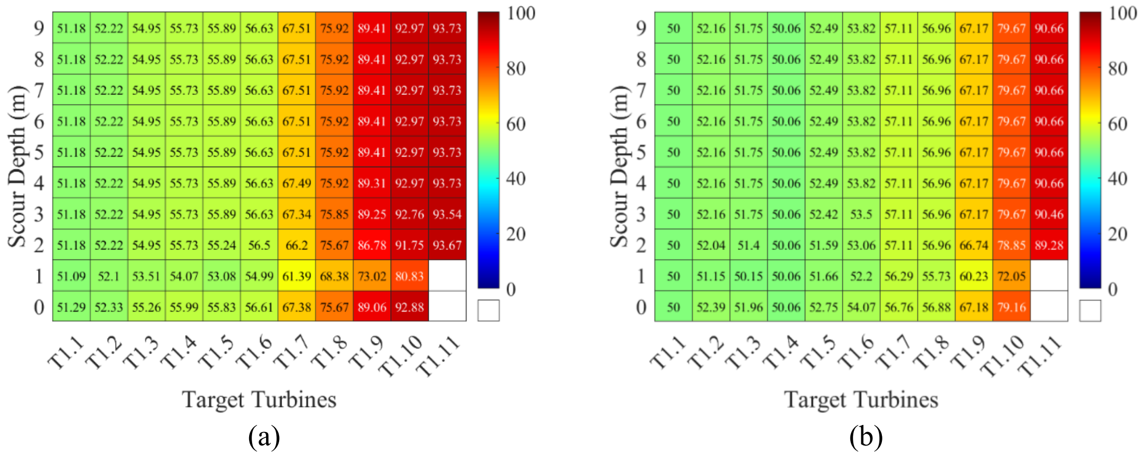

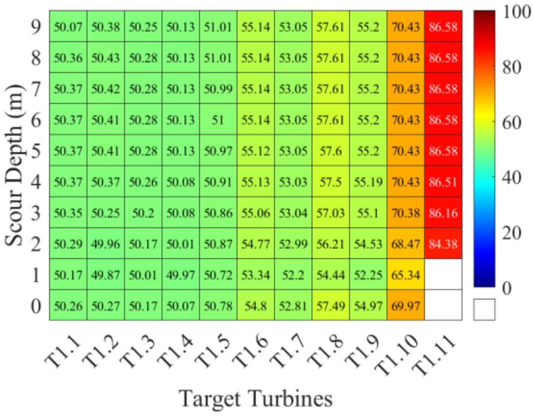

(c)

Figure A3: The baseline model performance when trained on Task 3 and evaluated on target OWTs located at a) Farm 1, b) Farm 2, and c) Farm 3.

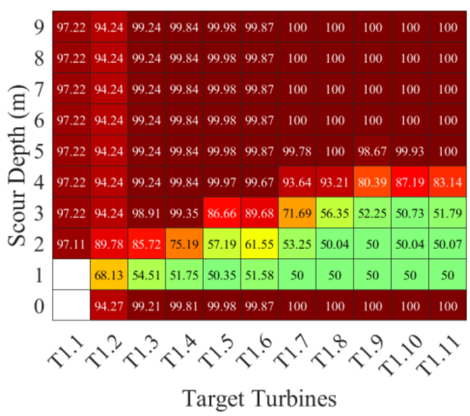

(a)

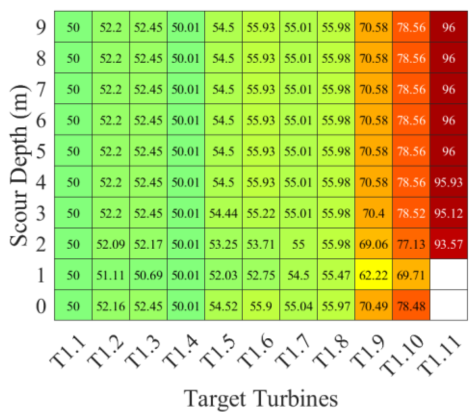

(b)

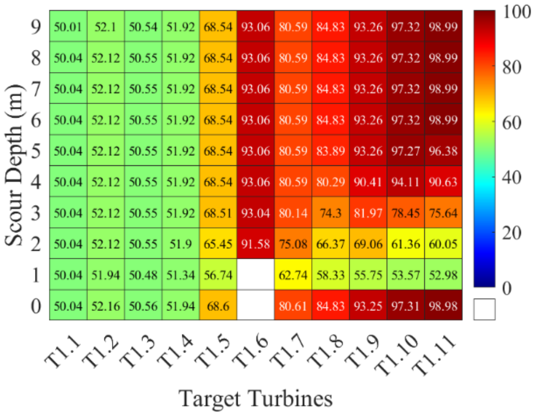

(c)

Figure A4: The baseline model performance when trained on Task 4 and evaluated on target OWTs located at a) Farm 1, b) Farm 2, and c) Farm 3.

Comment (2): Also very relevant, is the absence of any non-scour case: without it, we cannot say if the model can accurately distinguish between normal operation and scour, or if it's just triggering for different turbines because their dynamics are somewhat different from the training turbines'.

Reply to Comment (2): We agree that including the detection of non-scour (healthy) state is essential to demonstrate that the proposed framework distinguishes between healthy and scoured states of the monopile foundations, rather than being affected by the dynamic differences between OWTs located at multiple OWFs. To address this concern, the capability of the proposed DG model is assessed to detect the healthy (0m scour) condition by implementing the healthy state into the evaluation dataset for all unseen target turbines, evaluating the performance of the proposed framework accordingly. The revised results now include the prediction performance for both healthy and scoured conditions, confirming the reliability of the proposed model to identify the healthy operating condition while maintaining its capability to distinguish different scour states across previously unseen target turbines. The study findings indicate that the proposed model learns scour-related features that generalise across different OWFs and are not affected by the variations in turbine-specific dynamic characteristics.

A paragraph of text has been added to the revised manuscript, shown in blue text. For convenience, this is also shown below. (Relevant text from manuscript Section 4.1, lines 550-570)

Figure 1a-6c illustrate the performance of the proposed model in identifying the scour state at target turbines in Farms 1, 2, and 3, respectively. The robustness of the proposed framework is assessed by evaluating its capability to detect the healthy condition, which verifies the model's capacity to distinguish normal operating conditions from scour-induced foundation degradation. The results show that the proposed DG framework accurately identifies healthy foundation conditions while maintaining reliable prediction performance for the different scour depths across previously unseen target turbines. For example, the model effectively detected the healthy state for all target turbines across different wind farms when training using Task 1. In addition, the results indicate that in Task 1, the model effectively detects scour states with scour depths ($S > 3$ m, $S/D > 0.5$) around monopile foundations in Farm 1 and Farm 2. Whereas its performance is reduced at Farm 3, particularly for the deep-water units (T3.8–T3.11). Although performance decreases for shallow scour depths ($S = 1 - 3$ m, $S/D = 0.167 - 0.5$), the model reliably detects intermediate scour ($S = 4 - 6$ m, with $S/D = 0.67 - 1.0$) and deep scour levels ($S = 7 - 9$m, with $S/D > 1$) across the studied farms. Overall, Task 1 demonstrates high robustness in consistently detecting scour depths across various turbines, regardless of their site-specific conditions. The classification performance shown in Figure 1 represents the prediction accuracy for each scour condition and does not imply a direct linear relationship between scour depth and detection performance. Increasing scour depth leads to greater modification of the soil–structure interaction system and consequently larger changes in the turbine dynamic response. As scour depth increases, the foundation stiffness decreases, resulting in a more flexible support system. Initially, the structural response is dominated by bending behaviour; however, as scour progresses, the response may gradually transition towards a more rigid-body rotational mode. Consequently, the incremental changes in the dynamic characteristics become smaller with increasing scour depth, potentially making the detection of deeper scour levels more challenging. This trend is also reflected in the diminishing rate of increase in the natural period (or corresponding reduction in natural frequency) as scour depth continues to increase.

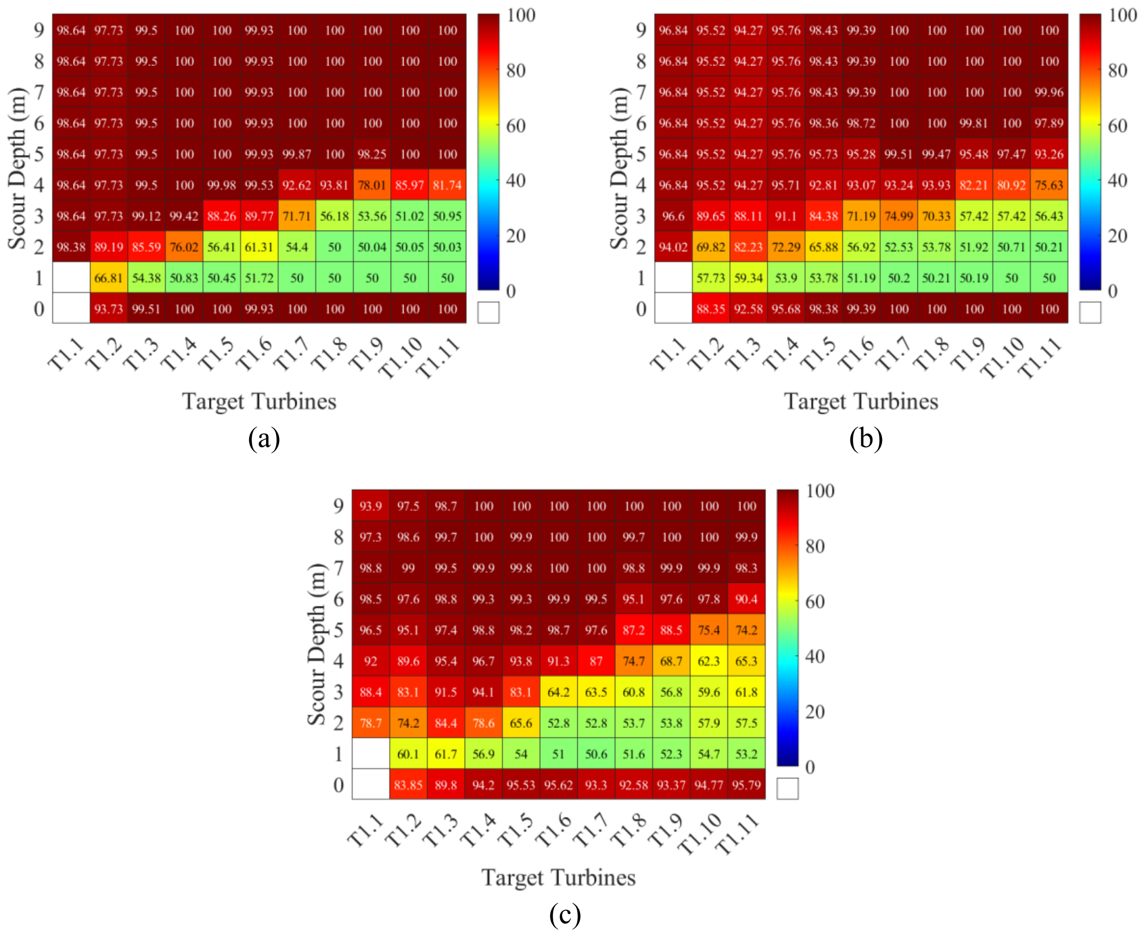

Figure 1: The proposed model performance when trained on Task 1 and evaluated on target OWTs located at a) Farm 1, b) Farm 2, and c) Farm 3.

Figure 2a- 7c illustrate the model's performance when trained on Task 2 and evaluated on the remaining target turbines across the given farms. As shown, the model achieves satisfactory performance for detecting the healthy state at turbines located in deeper water depth and with higher soil density when training using Task 2. However, the model fails to detect the healthy state for turbines located in shallower water depth and with lower soil density. This demonstrates that the learned representations are associated with scour-induced changes in structural dynamics rather than turbine-specific characteristics arising from differences in foundation properties, structural configuration, or environmental conditions. In Task 2, the model exhibits low generalisation capability across wind farm units, with satisfactory accuracy limited to turbines closely matching the source conditions, particularly in terms of water depth and soil density. A similar trend is observed across all three wind farms, where turbines located at greater water depths than the source turbine are accurately identified. In contrast, the scour detection performance degrades for turbines in shallower water due to the distributional shift in data caused by differences in water depth and soil stiffness. These shifts lead to misclassification, with the model often incorrectly identifying a healthy state as scoured due to similarities between the source turbines' healthy state and the target turbines' scoured state. Despite its limited performance for shallow water turbines (T1.1 – T1.5, T2.1 – T2.5, and T3.1 – T3.5), the model effectively detects scour in deep-water turbines, achieving accuracies above 90%.

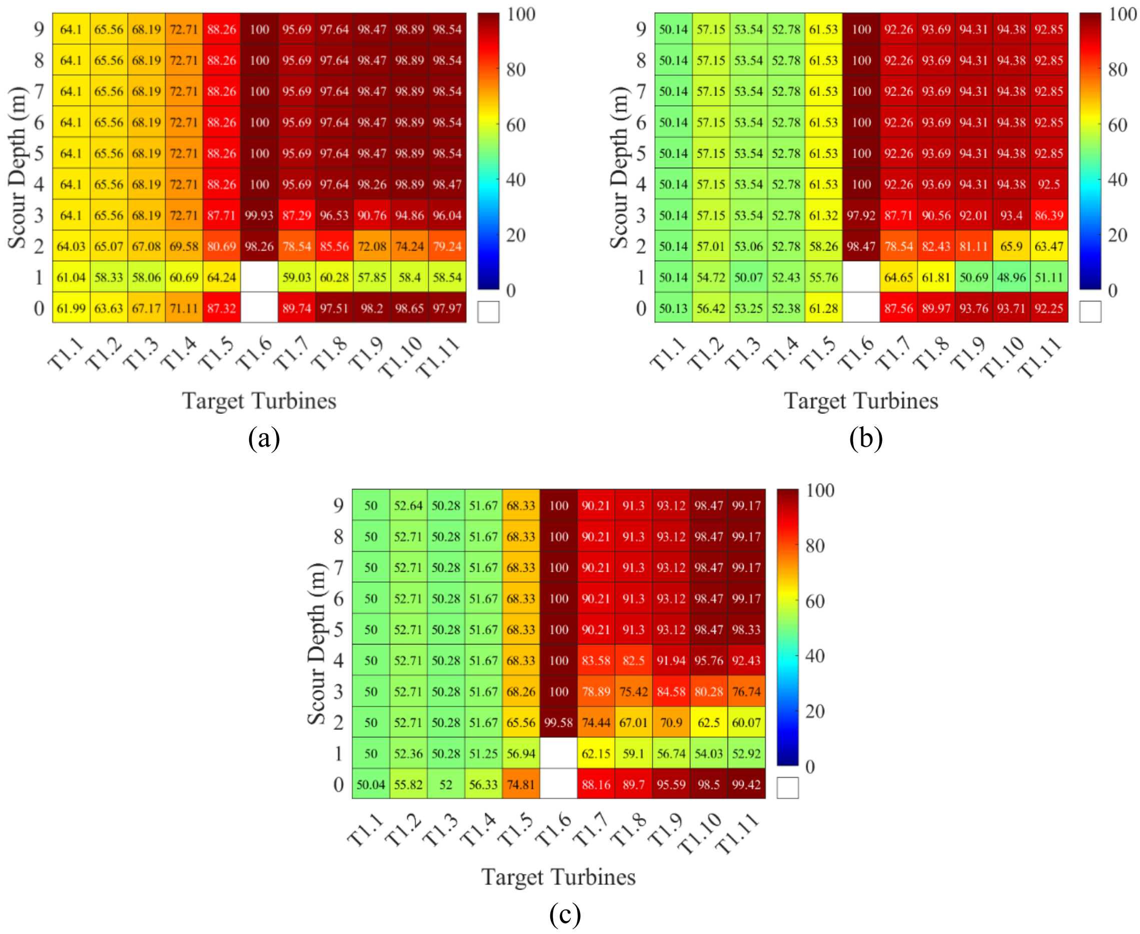

Figure 2: The proposed model performance when trained on Task 2 and evaluated on target OWTs located at a) Farm 1, b) Farm 2, and c) Farm 3

Figure 3a- 8c indicate the model accuracy when trained on Task 3 and evaluated on the remaining turbines across all three farms. When trained using Task 2, the model demonstrates satisfactory capability in identifying the healthy state for turbines operating in deeper water depths and characterised by higher soil densities. However, its performance deteriorates for turbines located in shallower water depths and softer soil conditions, where the healthy state is not reliably detected. The results show that model performance is strongly influenced by the source turbine location within each farm. Notably, scour detection at Farm 1 yields the most consistent results compared with Farms 2 and 3. The model achieves acceptable accuracy for the four turbines closest to the source (T1.9–T1.11); however, its accuracy drops sharply for turbines in shallower water, indicating limited generalisation across target turbines operating under varying conditions. This reduction in accuracy is primarily due to differences between the invariant features learned during training and those observed during evaluation. A comparison across the different training tasks further reveals that using shallow-water turbines with lower soil stiffness as source domains consistently outperforms training on intermediate- or deep-water turbines with higher soil stiffness, indicating the importance of carefully selecting source turbines to maximise scour detection performance at the wind farm scale.

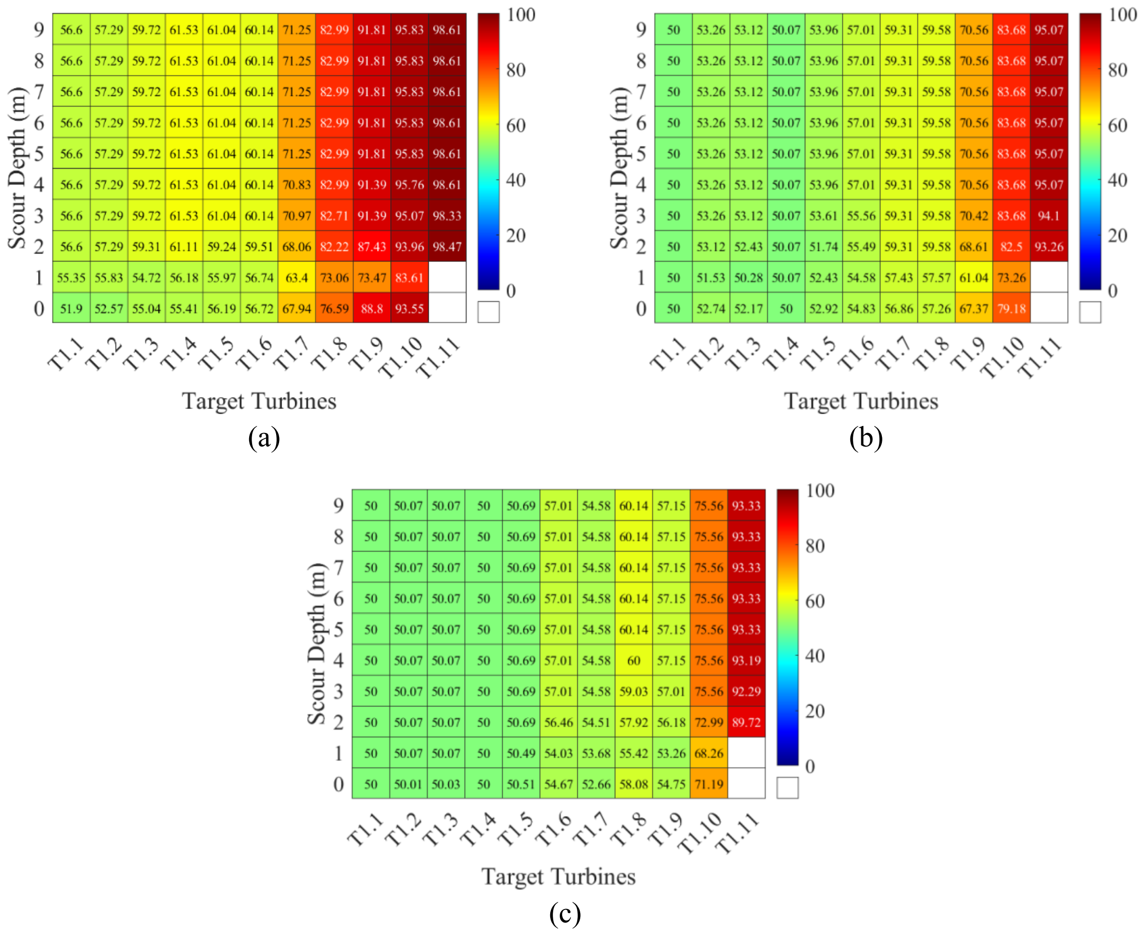

Figure 3: The proposed model performance when trained on Task 3 and evaluated on target OWTs located at a) Farm 1, b) Farm 2, and c) Farm 3

Figure 4a- 9c represent the results for the model's capacity trained on Task 4, and assessed across multiple target turbines. As shown, the model demonstrates strong capability in identifying the healthy state for Farm 1; however, its performance deteriorates when applied to Farms 2 and 3. In these cases, satisfactory detection is achieved only for turbines located in deeper waters, while the accuracy decreases significantly for turbines operating in shallower water conditions. The results demonstrate that models trained on combined source data achieve higher scour-detection accuracy when shallow-water turbines with lower soil density are employed as source domains. In contrast, performance decreases when intermediate or deep-water turbines with increased soil density are selected. This reduction in accuracy is primarily attributed to the model's limited capability to identify the healthy state, which is misclassified as scour due to distributional shifts. Overall, the model reliably detected scour for turbines installed at greater water depths, particularly those with higher soil stiffness than the training conditions. Consequently, the proposed framework exhibits improved generalisation capability for practical deployment across heterogeneous OWFs, where both healthy and scoured foundation conditions are expected to coexist. Despite its enhanced performance in detecting healthy state when only healthy data exist at the unseen turbine, its performance reduced sharply for detecting 1-2m scour depth due to the reduced impact on the dynamic performance leads to small changes due to scour is masked by operational and environmental variation.

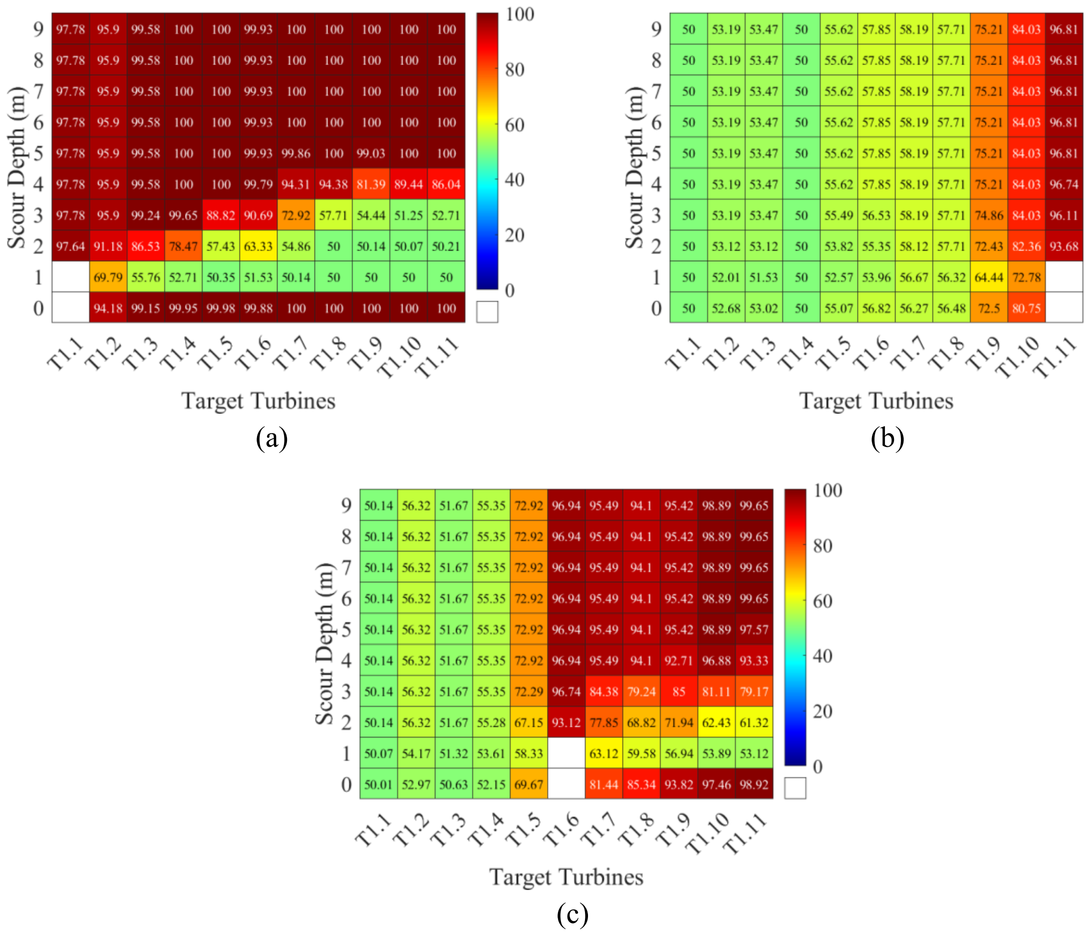

Figure 4: The proposed model performance when trained on Task 4 and evaluated on target OWTs located at a) Farm 1, b) Farm 2, and c) Farm 3

Comment (3): Therefore, the conclusion that model training is best performed for the shallowest farms/turbines with lowest stiffness foundation could be called into question (if, i.e., the model is just triggering in different dynamics and not on actual scour). Given this assertion, it could also be considered as an additional baseline into the 'population-based' approach to train in a single turbine (e.g. T1.1., the shallowest and with lowest soil stiffness).

Reply to Comment (3): Comparing the proposed multi-source DG-based training strategy with a model trained using single source turbine is implemented in the revised manuscript to assess the advantages of combining multiple source turbines. Additional analysis has been conducted in which the model is trained exclusively using Turbine 1.1, corresponding to the shallowest water depth and lowest foundation stiffness, and subsequently evaluated on the same set of previously unseen target turbines. The results are compared directly with those obtained using the proposed DG-based multi-source training framework. The comparison demonstrates that although the single-turbine model trained on Turbine 1.1 achieves competitive performance, particularly for target turbines located at Farm 1 with similar dynamic characteristics, its prediction accuracy deteriorates for turbines exhibiting larger variations in soil properties, water depths, and structural configurations, located at other wind farms (Farm 2 and 3). The model fails to detect any scour state at any turbines located at these farms, where mostly healthy state are misclassified as scour or vice versa. In contrast, the proposed DG-based framework consistently provides superior prediction accuracy and improved robustness across all evaluation scenarios. By exposing the model to a broader range of operating conditions and structural characteristics during training, the multi-source strategy enables the learning of more representative and domain-invariant scour-related features, thereby improving generalisation to previously unseen OWTs. The additional study findings further confirm the improved performance of the proposed framework corresponding to selecting a favourable source turbine and increased diversity of the training data used for training the DG model.

A paragraph of text has been added to the revised manuscript, shown in blue text. For convenience, this is also shown below. (Relevant text from manuscript Section 4.1, lines 590-605)

To further evaluate the effectiveness of the proposed DG-based training strategy, an additional baseline is considered in which the model is trained exclusively using data from Turbine 1.1, representing the shallowest water depth and lowest foundation stiffness among the investigated OWTs. Figure 5 represents the performance of the single-source DG model, developed using the PSD features extracted from the acceleration responses of Turbine 1.1 under healthy and 1 m scour conditions. The model is evaluated for scour-state detection across multiple target turbines located in Farms 1, 2, and 3. Compared with that of the proposed DG-based framework using the same unseen target turbines, the single-source model achieves satisfactory results for detecting the scour state at the same farm (Farm 1). However, in terms of its performance in detecting scour at Farm 2, its capability to detect scour deteriorates significantly at other farms (Farm 2 and 3), failing fully to detect any scour scenario at any target turbines within these farms. Although the single-source model achieves satisfactory performance for turbines with similar dynamic characteristics, its prediction accuracy decreases as the discrepancy between the source and target turbines increases. In contrast, the DG-based framework consistently demonstrates improved prediction accuracy and robustness across the diverse target turbines. These findings indicate that the enhanced performance of the proposed framework is primarily attributed to the increased diversity of the source-domain data, which enables the model to learn more generalised scour-related features, rather than relying on the characteristics of a single favourable source turbine.

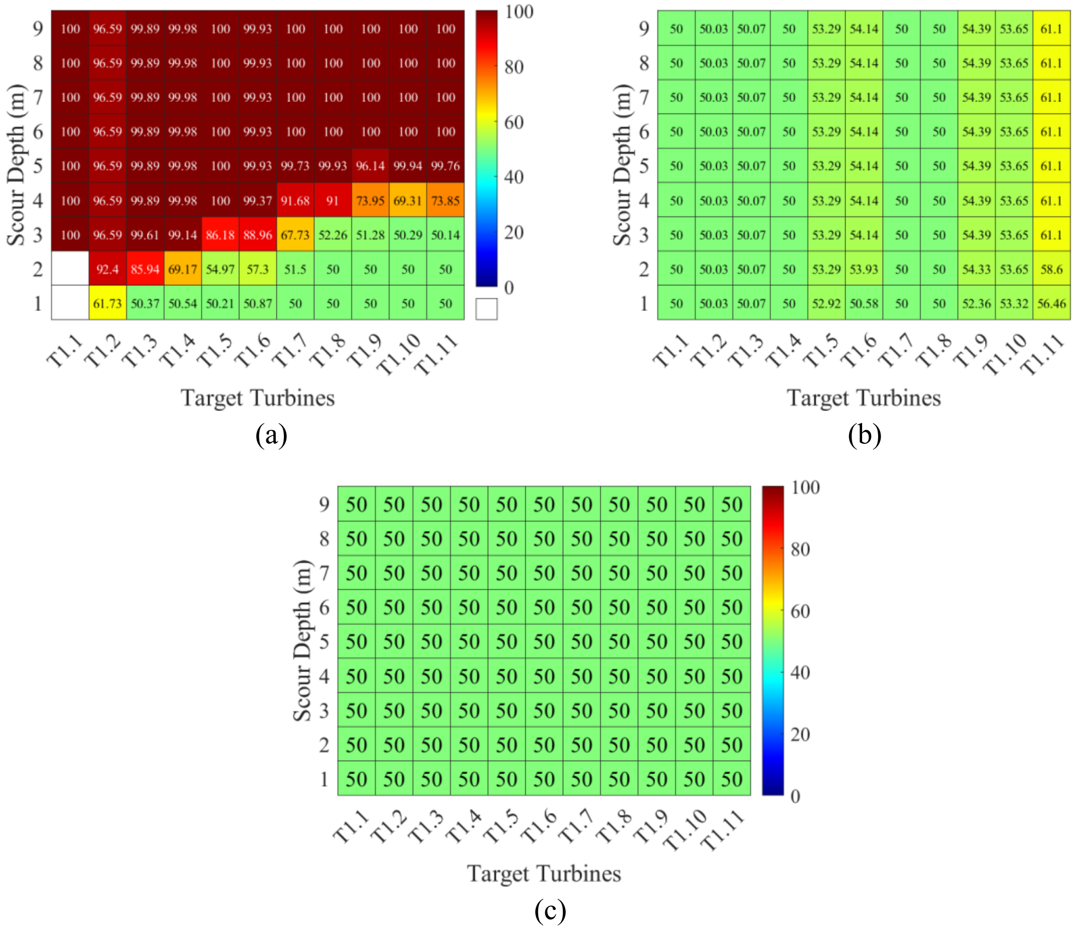

Figure 5: the performance of a single model when trained on turbine T1.1 and evaluated on target OWTs located at a) Farm 1, b) Farm 2, and c) Farm 3

Comment (4): A further suggestion related to this conclusion would be to fully flesh it out in terms of what it means for the structures' eigenfrequency (lower soil density, lower stiffness, lower eigenfrequency, but conversely, shallower water depth, higher eigenfrequency).

Reply to Comment (4): To address this comment, an additional parametric investigation has been conducted to independently examine the influence of soil density and water depth on the natural frequencies of the OWTs. Specifically, the effect of varying the soil density across wind farms while maintaining a constant water depth, as well as the effect of a regular increase in water depth and slight soil variations within a specific wind farm as shown in Table 3. This approach enables the individual contributions of foundation stiffness and structural geometry to be distinguished. The results confirm that decreasing the soil density across wind farms reduces the lateral foundation stiffness, leading to a corresponding reduction in the natural frequencies of the turbine-foundation system. Similarly, increasing water depth further increases the unsupported tower height and structural flexibility, resulting in a further increase in the natural frequencies. This explains the favourable characteristics of using turbines installed in shallow water with relatively compliant foundation conditions as source turbines, as they encompass a broader range of dynamic behaviour that improves the model's ability to generalise across diverse target turbines.

A paragraph of text has been added to the revised manuscript, shown in blue text. For convenience, this is also shown below. (Relevant text from manuscript Section 3.5, lines 410-455)

The influence of scour-induced modal characteristic changes is assessed through investigating the data distribution for OWT in both healthy and scoured states using the MMD. The results show that the MMD distance between healthy and scoured conditions increases with scour depth, reflecting the increasing deviation in the dynamic response caused by foundation stiffness degradation. In contrast, variations in soil density between healthy turbines introduce significant domain shifts, as observed from the increased MMD values between turbines located at different farms. These shifts become more pronounced when variations in soil conditions are combined with changes in water depth, further increasing the discrepancy between source and target turbine responses. These results highlight the challenge of scour detection under realistic offshore conditions. Small scour-induced frequency shifts may be difficult to distinguish from normal operational variability and site-to-site differences, whereas larger domain shifts can cause healthy-state responses from one turbine or farm to overlap with scoured-state responses from another. Therefore, effective scour detection requires a DG framework capable of identifying scour-related dynamic changes while reducing sensitivity to non-damage-related variations.

To further investigate the physical influence of scour on the turbine dynamic response, the natural frequencies of the healthy and scoured foundation conditions are estimated from the simulated acceleration responses using the Frequency Domain Decomposition (FDD) method. Table 1 shows the natural frequencies for the first four bending modes as well as the rate of variation/ reduction under different scour states (3m, 6m, and 9m scour depth) based on healthy state measurements. It represents the natural frequencies for different turbines, characterised with various water depths and soil densities (T1, T6, and T11) across different wind farms. The results demonstrate that increasing scour depth leads to a reduction in the effective foundation stiffness due to the progressive loss of soil support, resulting in a decrease in the tower natural frequencies. Specifically, the first bending natural frequency shows a negligible impact due to scour severity progression. However, the 2nd mode shows increased impact, where it decreases from 1.422Hz for the healthy condition to 1.081Hz for the maximum considered scour depth of 9m, corresponding to a frequency reduction of 24%. The magnitude of this frequency shift increases consistently with scour severity, confirming that scour-induced degradation of the soil–foundation system directly modifies the global dynamic characteristics of the offshore wind turbine. The effect of increasing the scour severity on the dynamic response of multiple turbines within different wind farms is assessed. In addition, decreasing the soil density while keeping the water depth constant leads to further reduction in the natural frequencies (1.422Hz for T1.1, 1.24Hz for T2.1, and 1.148Hz for T3.1). A similar trend is noticed for higher-order frequencies. Increasing the water depth leads to slight variation in natural frequencies compared with those caused by changes in soil properties. At a constant water depth of 20m, reducing soil density at turbines T1.1, T2.1, and T3.1 decreases the lateral foundation stiffness, increasing the flexibility of the soil–foundation system and consequently reducing the natural frequencies. In contrast, greater water depths increase the unsupported tower height and global structural flexibility, with more pronounced effects observed at higher-order modes. The first-order natural frequency, however, shows negligible variation with turbine location or scour state. Specifically, 2nd order mode natural frequency shows the highest reduction due to scour depth increase. This trend is consistent across different turbines within the wind farm. These observations indicate that both soil stiffness and water depth significantly influence the dynamic characteristics of OWTs, which enables the selection of representative source turbines to enhance the model generalisation capacity.

Table 1: First four bending mode natural frequencies of healthy and scoured turbines across different farms

		Damage Condition				Percentage of change		
Turbine	**Mode**	**Healthy (Hz)**	**3m (Hz)**	**6m (Hz)**	**9m (Hz)**	**3m (%)**	**6m (%)**	**9m (%)**
T1.1	1st mode	0.244	0.244	0.244	0.244	0.0	0.0	0.0
	2nd Mode	1.422	1.337	1.210	1.081	6.0	14.9	24.0
	3rd Mode	2.909	2.844	2.705	2.611	2.2	7.0	10.2
	4th Mode	6.595	6.479	6.273	6.116	1.8	4.9	7.3
T1.6	1st mode	0.246	0.246	0.244	0.244	0.0	0.8	0.8
	2nd Mode	1.399	1.337	1.210	1.131	4.4	13.5	19.2
	3rd Mode	2.992	2.916	2.781	2.659	2.5	7.1	11.1
	4th Mode	6.755	6.568	6.411	6.097	2.8	5.1	9.7
T1.11	1st mode	0.244	0.244	0.244	0.244	0.0	0.0	0.0
	2nd Mode	1.422	1.348	1.210	1.148	5.2	14.9	19.3
	3rd Mode	3.095	3.019	2.844	2.746	2.5	8.1	11.3
	4th Mode	6.866	6.758	6.500	6.273	1.6	5.3	8.6
T2.1	1st mode	0.248	0.248	0.244	0.244	0.0	1.6	1.6
	2nd Mode	1.244	1.210	1.140	1.100	2.7	8.4	11.6
	3rd Mode	2.792	2.732	2.652	2.568	2.1	5.0	8.0
	4th Mode	6.416	6.292	6.150	6.039	1.9	4.1	5.9
T2.6	1st mode	0.248	0.248	0.248	0.244	0.0	0.0	1.6
	2nd Mode	1.228	1.159	1.064	1.100	5.6	13.4	10.4
	3rd Mode	2.791	2.752	2.650	2.568	1.4	5.1	8.0
	4th Mode	6.405	6.260	6.098	6.039	2.3	4.8	5.7
T2.11	1st mode	0.244	0.244	0.244	0.244	0.0	0.0	0.0
	2nd Mode	1.324	1.210	1.164	1.092	8.6	12.1	17.5
	3rd Mode	2.945	2.881	2.801	2.698	2.2	4.9	8.4
	4th Mode	6.561	6.518	6.308	6.163	0.7	3.9	6.1
T3.1	1st mode	0.244	0.244	0.244	0.244	0.0	0.0	0.0
	2nd Mode	1.148	1.099	1.047	0.968	4.3	8.8	15.7
	3rd Mode	2.661	2.617	2.542	2.450	1.7	4.5	7.9
	4th Mode	6.212	6.108	6.029	5.972	1.7	2.9	3.9
T3.6	1st mode	0.244	0.244	0.244	0.244	0.0	0.0	0.0
	2nd Mode	1.210	1.132	1.074	1.011	6.4	11.2	16.4
	3rd Mode	2.737	2.687	2.642	2.542	1.8	3.5	7.1
	4th Mode	6.293	6.212	6.044	6.029	1.3	4.0	4.2
T3.11	1st mode	0.248	0.248	0.248	0.235	0.0	0.0	5.2
	2nd Mode	1.210	1.159	1.098	1.024	4.2	9.3	15.4
	3rd Mode	2.820	2.790	2.714	2.628	1.1	3.8	6.8
	4th Mode	6.365	6.283	6.162	6.070	1.3	3.2	4.6

Error! Reference source not found. represents the PSD for turbines (T1.1, T2.1, T3.1) in both healthy and scoured states at the 0-8Hz range, with the frequency ranges corresponding to the first, second, third, and fourth modes highlighted. As shown, the first-mode natural frequency exhibits the smallest variation with changes in scour condition and turbine location. In contrast, higher modes, particularly the second mode, exhibit greater sensitivity to changes in scour condition, along with additional variations associated with turbine location. A similar trend is expected for the higher modes, including the third and fourth modes.

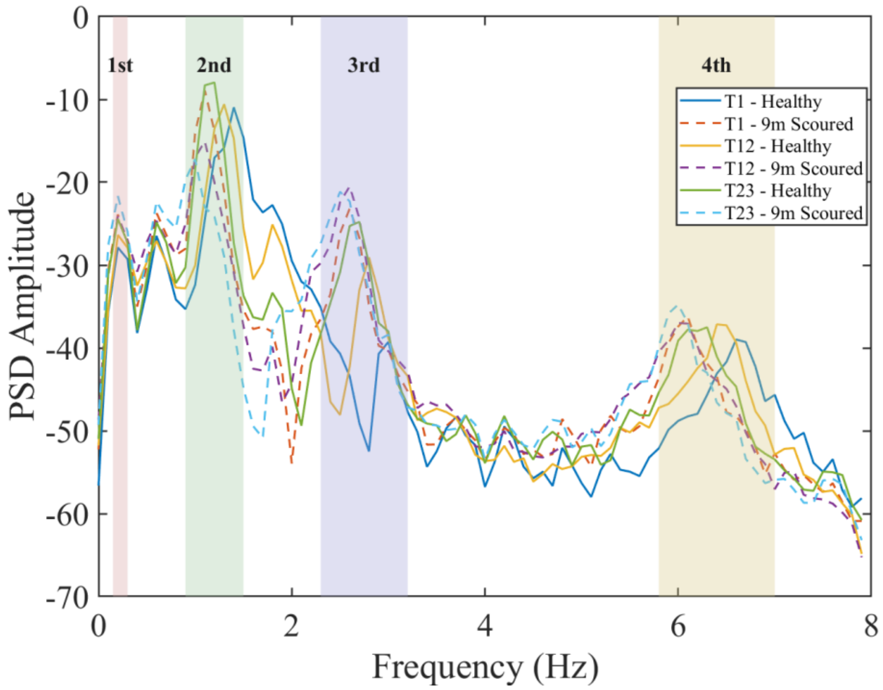

Figure 6: **PSD for turbines (T1.1, T2.1, T3.1) in both healthy and scoured states at the 0-8Hz range**

Comment (5): The setup of the experiment could also be strengthened in the introduction: in a landscape where there are few labelled scour data (and therefore an incentive for self-supervised learning) and OWT fleets more often than not consist of different wind turbine types, how would you set up the current experiment? These aspects could also be reflected in the conclusions/future work.

Reply to Comment (5): The practical deployment of machine learning-based scour monitoring systems is constrained by the limited availability of labelled scour data and the increasing heterogeneity of OWT fleets. These considerations provide important motivation for developing models that can generalise at different turbines across multiple wind farms and operating environments. The proposed DG-based scour detection framework represents an important step towards scalable fleet-wide scour monitoring. Although the current work assumes the availability of labelled data from representative source turbines to investigate cross-farm generalisation, this assumption reflects realistic inspection practices in which a limited number of turbines can be monitored and labelled through periodic inspections or numerical simulations. The proposed framework is therefore intended to maximise the utilisation of these limited labelled datasets by enabling knowledge transfer to previously unseen turbines without requiring target-domain labels. Furthermore, the Conclusions and future work sections have been revised to highlight that future research will investigate self-supervised and semi-supervised learning strategies to further reduce the dependence on labelled scour data. In addition, extending the framework to heterogeneous offshore wind fleets comprising different turbine ratings, manufacturers, and foundation configurations has been identified as an important direction towards practical industrial deployment.

A paragraph of text has been added to the revised manuscript, shown in blue text. For convenience, this is also shown below. (Relevant text from manuscript Section introduction, lines 80-100)

This challenge is particularly pronounced in OWTs, where acquiring labelled scour data is inherently difficult. In addition, scour develops gradually over time, while underwater inspections are expensive, infrequently scheduled, and dependent on the availability of specialised inspection vessels and professional divers. Moreover, direct acceleration measurements of source or target foundations are rarely available, making the collection of representative labelled datasets both costly and impractical in many operational conditions, as collecting reliable damage labels requires direct knowledge of the structural condition of the OWT. Consequently, only a limited number of turbines are expected to possess reliable labelled datasets, whereas the majority of the turbine fleet is likely to remain unlabelled. Furthermore, modern OWFs frequently comprise turbines operating under various structural configurations and site-specific environmental and geotechnical conditions, resulting in significant domain shifts between individual turbines. In addition, the differences between turbines in water depth, soil properties, foundation characteristics, and environmental loading can significantly alter the structural dynamic response, constraining the generalisation capability of conventional data-driven ML models trained on a single turbine or site.

To address this challenge, this study proposes a multi-source domain generalisation (DG) -based scour detection framework that learns domain-invariant feature representations consistent across multiple OWFs. This is conducted through transferring the knowledge from a limited number of labelled turbines to previously unseen target turbines without requiring additional target-domain labels.

A paragraph of text has been added to the revised manuscript, shown in blue text. For convenience, this is also shown below. (Relevant text from manuscript Section 4.4, lines 680-685)

Although the proposed framework demonstrates effective cross-farm scour detection using labelled data from representative source turbines, future research should investigate learning strategies that further reduce the reliance on labelled data. In particular, self-supervised and semi-supervised learning approaches offer considerable potential for exploiting the large volumes of unlabelled operational monitoring data routinely collected from OWTs. Furthermore, extending the proposed framework to heterogeneous offshore wind fleets comprising different turbine ratings, manufacturers, support structures, and foundation types represents an important step towards scalable fleet-wide structural health monitoring and practical industrial deployment.

Comment (6): Regarding the modelling in OpenFAST in sections 2.3. and 3., more details could be provided:

- How long is the simulated time period?
- How much time was cut off as an initialisation period?
- Which turbulence model or intensity was used for the wind field?
- Which wave spectrum was used?
- How was SSI modelled? soil-springs? linear or non-linear? PISA or API p-y?
- How was scour included in the model?
- Some further clarifications could also be provided:

Reply to Comment ( ): We agree that additional details regarding the numerical modelling are essential to improve the clarity and reproducibility of the study.

To address this comment, Sections 2.3 and 3 have been revised to provide a more comprehensive description of the OpenFAST simulations and the coupled soil–structure interaction (SSI) model. The revised manuscript now specifies the simulation duration, the discarded initial transient period, the wind turbulence model and turbulence intensity, the wave spectrum adopted for hydrodynamic loading, the SSI modelling approach, and the procedure used to represent scour within the numerical model. These additions provide a more complete description of the numerical framework and facilitate the reproducibility of the proposed methodology.

A paragraph of text has been added to the revised manuscript, shown in blue text. For convenience, this is also shown below. (Relevant text from manuscript Section 3.3, lines 307-310)

It is important to note that this study does not take yaw misalignment into account, which enables the analysis to concentrate only on changes in the dynamic response occurring due to the scour effect. Specifically, each simulation is performed for a total duration of 3700 s, with the initial 100 s discarded to eliminate transient effects associated with model initialisation. The simulation implemented a time step of 0.001 s, while the response outputs at every 0.01 seconds.

A paragraph of text has been added to the revised manuscript, shown in blue text. For convenience, this is also shown below. (Relevant text from manuscript Section 3.3, lines292 - 307)

The dynamic response of each OWT is simulated using the aero-hydro-servo-elastic solver OpenFAST for the NREL 5 MW reference turbine model under combined aerodynamic and hydrodynamic loading.

Turbulent wind fields are generated using TurbSim based on the IEC Kaimal turbulence model (IECKAI) (Cheynet et al., 2017), as recommended by the IEC 61400-1 standard for simulating atmospheric turbulence acting on wind turbines. A Normal Turbulence Model (NTM) with IEC turbulence class B and a turbulence intensity of 12% was adopted to represent typical offshore operating conditions. The mean wind speed at the reference height of 90 m was specified based on the defined environmental conditions in Section 3.2, while the vertical wind profile was modelled using the IEC power-law formulation. The resulting stochastic wind field captures the spatial and temporal fluctuations of atmospheric turbulence across the rotor plane, providing realistic aerodynamic loading for the OpenFAST simulations. Multiple stochastic wind conditions were generated for each turbine and environmental condition to capture the variability associated with turbulent loading. The wake effect was included in the OpenFAST Aerodyne module using the Blade Element Momentum (BEM) Theory. In addition, the irregular wave conditions are represented using the JONSWAP spectrum incorporated in OpenFAST, with the corresponding significant wave height and peak wave period defined according to the environmental conditions considered for each OWF, as indicated in Section 3.2. Aerodynamic loads are computed using Blade Element Momentum theory (Zhao et al., 2019), whereas hydrodynamic loads acting on the support structure are evaluated using Morison's equation (Wolfram & Naghipour, 1999). The sea current is incorporated using the normal current model.

A paragraph of text has been added to the revised manuscript, shown in blue text. For convenience, this is also shown below. (Relevant text from manuscript Section 3.3, lines 311-342)

This study particularly focuses on evaluating the influence of domain shifts arising from environmental, geotechnical, and structural variations on scour detection performance. A fixed random seed is used for all OpenFAST simulations to ensure reproducibility and maintain consistency in the generation of stochastic environmental conditions, including wind and wave realisations. This ensures identical turbulent wind realisations were generated, allowing changes in the structural response to be attributed solely to the investigated scour conditions rather than variations in the environmental loading. This assumption is considered appropriate for evaluating the domain generalisation capability of the proposed framework, where the objective is to capture variations arising from different turbine and foundation characteristics rather than farm-level aerodynamic interactions. Variations in operational and site conditions are incorporated into both training and testing datasets to represent realistic OWT operating scenarios. The integration of these factors with SSI and turbine dynamic characteristics provides a comprehensive framework for representing realistic OWT behaviour. By incorporating site-specific operational conditions, the scenarios/ tasks defined in Section 2.5 are used to train, evaluate and validate the capability of the proposed framework to detect scour across multiple OWF environments under realistic operating conditions. In addition, variations in water depth, soil properties, turbine characteristics, and scour depth are considered to represent the heterogeneous conditions encountered across OWFs. The integration of these factors with SSI and turbine dynamic characteristics provides a comprehensive framework for representing realistic OWT behaviour. These variations ensure that the ML model is exposed to a wide range of dynamic responses associated with different turbine and foundation configurations.

Although the dynamic characteristics of OWTs are influenced by various factors, including environmental variability, soil–structure interaction conditions, and structural degradation mechanisms such as corrosion, marine growth, settlement, and grout deterioration, this study focuses exclusively on scour-induced changes resulting from reductions in foundation stiffness and modifications to boundary conditions. Accordingly, the proposed framework is intended to detect scour-related variations in the turbine's bending modal characteristics rather than serve as a universal diagnostic tool for all degradation mechanisms. Other operational uncertainties, including controller effects, rotor imbalance, sensor installation errors, measurement noise, and wake interactions between turbines in a wind farm, are not explicitly considered in the present numerical framework. The numerical simulations considered in this study primarily represent above-rated operating conditions, where the rotor speed is maintained close to the rated value through the turbine control system. Therefore, the 3P excitation frequency remains relatively consistent among the investigated turbines. However, the proposed scour detection framework does not rely on rotor harmonic components as the primary indicator of scour. Instead, it exploits changes in the global dynamic response of the OWT system resulting from variations in SSI performance and foundation stiffness. Above-rated operation represents an important condition for OWT monitoring because turbines frequently operate under these conditions during their service life. Nevertheless, extending the dataset to incorporate below-rated and transient operating conditions, where rotor speed and aerodynamic excitation vary significantly, represents an important direction for future research to evaluate the robustness and applicability of the proposed framework.

A paragraph of text has been added to the revised manuscript, shown in blue text. For convenience, this is also shown below. (Relevant text from manuscript Section 3.3, lines 343-370)

As OpenFAST assumes a rigid foundation and does not explicitly model SSI, a bespoke SSI model is developed in MATLAB and incorporated in OpenFAST by generating equivalent stiffness for zero-dimensional (0D) ground springs. The monopile foundation is represented using a modified Winkler formulation approach (Prendergast & Gavin, 2016), comprising distributed nonlinear lateral $p-y$ springs together with rotational $(m-\theta)$ and pile-tip springs to capture the flexibility of the pile–soil system (Tott-Buswell et al., 2024). The nonlinear soil resistance is derived from Cone Penetration Test (CPT)-based geotechnical properties using a modified $p-y$ approach, while the rotational resistance accounts for shaft-friction mobilisation generated during pile rotation (Byrne et al., 2015). The nonlinear load–displacement and moment–rotation responses are first evaluated in MATLAB under the mudline loading obtained from an equivalent rigid-foundation OpenFAST simulation. Equivalent lateral and rotational secant stiffnesses are then calculated and implemented in OpenFAST as zero-dimensional (0D) ground springs at the mudline. Consequently, although the underlying soil model is nonlinear, it is incorporated into OpenFAST through equivalent secant stiffness coefficients implemented as zero-dimensional (0D) ground springs at the mudline, resulting in a computationally efficient decoupled representation of foundation flexibility. To simulate the scoured conditions, the soil layer equivalent to the scour depth is removed, and the stiffness of the soil springs located within the scoured region is assigned to zero, effectively reducing the pile embedment and updating the foundation stiffness matrix. The updated equivalent stiffness matrix is then implemented in OpenFAST to simulate the dynamic response of the turbine under each scour condition. In this study, scour is characterised by scour depth, which represents the primary parameter influencing the loss of foundation stiffness and the resulting changes in turbine dynamic response. Other scour-hole geometrical parameters, such as scour width and slope angle, are not considered, as their influence on the global dynamic characteristics of the turbine is comparatively limited. This study covers nine scour states, each represented by a specific scour depth, with scour depths ranging from 1 m to 9 m (corresponding to S/D = 0.167–1.5) considered. The decoupled sub-structuring approach implemented herein has previously been validated against monotonic pile pushover experiments (Tott-Buswell et al., 2024) and has been successfully applied in previous OpenFAST-based scour modelling studies (Abdelhak et al., 2025); and (Abdelhak et al., 2026). In addition, simplified homogeneous soil profiles are adopted to isolate the influence of global soil stiffness on the dynamic response of OWTs and to evaluate the proposed framework under controlled geotechnical conditions. Although layered soil stratification can influence scour development and foundation dynamics, its effect on modal characteristics is generally smaller than that resulting from substantial changes in overall soil stiffness (e.g., dense versus loose sand) (Zefzouf et al., 2025). Therefore, the proposed framework is expected to remain effective under layered soil conditions, although its performance may be influenced by the degree of soil heterogeneity and layer configuration.

Comment (7):

- Line 254: what is meant by PSD features;
- Line 256: The t-SNE visualization is of the model's latent space?
- Line 315: what's the mix between the classification and domain losses?

Reply to Comment (7): Additional clarification regarding the feature extraction process, the t-SNE visualisation, and the optimisation objective of the DANN framework is added. The revised manuscript now provides a detailed explanation of the extracted power spectral density (PSD) features. Furthermore, the description of the t-SNE analysis has been updated to clarify that the visualisation is performed using the raw input data. Finally, the formulation of the DANN loss function has been expanded to specify the contribution of the classification and domain-adversarial losses and the weighting factor used to balance the two objectives during training.

A paragraph of text has been added to the revised manuscript, shown in blue text. For convenience, this is also shown below. (Relevant text from manuscript Section Introduction, lines 100-102)

The proposed approach relies on vibration measurements acquired from a single accelerometer installed on an OWT tower, with Power Spectral Density (PSD) features derived from the measured acceleration signals serving as the input to the ML model.

A paragraph of text has been added to the revised manuscript, shown in blue text. For convenience, this is also shown below. (Relevant text from manuscript Section 2.1, lines 120-125)

The simulated tower acceleration responses are transformed into PSD representations, which characterise the distribution of vibration energy across the frequency spectrum and capture changes in the turbine dynamic behaviour caused by scour. The extracted PSD features are subsequently normalised and organised into batches to facilitate latent feature learning and serve as the input for model training. The proposed framework combines supervised deep learning with domain generalisation to learn scour-related representations from labelled source turbines and transfer this knowledge to previously unseen target turbines without requiring target-domain data during training.

A paragraph of text has been added to the revised manuscript, shown in blue text. For convenience, this is also shown below. (Relevant text from manuscript Section 3.4, lines 379-385)

The selected frequency range of 0-8 Hz captures the dominant structural responses of the turbine, including the first four global bending frequency modes affected by variations in foundation stiffness, as well as the dynamic response associated with scour development within the given wind farms. Although the rotor excitation frequency 1P is located at a much lower frequency range, the structural modes within 0-8Hz range contain important information regarding changes in the system dynamic behaviour. Therefore, the extracted spectral features within this frequency range provide physically meaningful indicators for identifying scour-induced degradation.

A paragraph of text has been added to the revised manuscript, shown in blue text. For convenience, this is also shown below. (Relevant text from manuscript Section 3.4, lines 389-390)

The t-SNE visualisation shown in **Error! Reference source not found.** is performed based on the raw input data without the application of the DG model. Therefore, the visualisation illustrates the distribution of the reduced-dimensional raw PSD features.

A paragraph of text has been added to the revised manuscript, shown in blue text. For convenience, this is also shown below. (Relevant text from manuscript Section 4.1, lines 469-480)

For the DANN framework, the training objective comprises two complementary components: a classification loss and a domain classification loss. The classification loss enables the model to accurately identify the scour state, while the domain classification loss encourages the learning of feature representations that are independent of the source domain, thereby reducing the influence of variations between turbines, sites, and operating conditions. During training, the classification branch learns to predict the scour state from the labelled source-domain data, whereas the domain discriminator learns to distinguish the domain from which each sample originates. At the same time, the feature extractor is optimised to improve scour classification performance while making the extracted features increasingly difficult for the domain discriminator to identify. This adversarial learning process encourages the model to retain information relevant to scour while suppressing domain-specific characteristics, resulting in feature representations that are both discriminative and transferable. Consequently, the trained model exhibits improved robustness under varying operating conditions and can be more effectively applied to previously unseen turbines and offshore wind farms.

Comment (8):

- Present scour depths as a fraction of the tower diameter (D). Naturally for some cases D varies, but the fraction makes results more interpretable.
- CDDG should first appear explained under the methodology and not in section 4.4.
- Add a column to Table 13 with a brief description of each task.
- Tables 3-12 could be in annex to improve readability and text flow.

Reply to Comment (8): The scour depth is expressed as a fraction of the monopile diameter (S/D, where S represents scour depth while D is the monopile diameter). Noting that the scour depth is usually described as a fraction of the monopile diameter not the tower. Furthermore, the description of the Causal Contextual Domain Generalisation (CCDG) method has also been revised. A detailed explanation of CCDG has been moved from Section 4.4 to the Methodology section, where all domain generalisation approaches are introduced consistently before presenting the comparative results. Moreover, Table 13 has been revised by adding a column describing the objective and characteristics of each training task to provide clearer context regarding the selection of source and target turbines. Finally, Tables 3–12, which contain detailed foundation specifications, environmental and operational conditions, as well as the MMD values for different scenarios, have been moved to the Appendix to improve the readability and flow of the main manuscript. The key findings and comparative discussions remain presented in the main text.

A paragraph of text has been added to the revised manuscript, shown in blue text. For convenience, this is also shown below. (Relevant text from manuscript Section 2.5, lines 229-232)

The scour depth is represented as a fraction of the monopile diameter to enable better interpretation of the results and account for variations in turbine and foundation dimensions among different wind farms.

A paragraph of text has been added to the revised manuscript, shown in blue text. For convenience, this is also shown below. (Relevant text from manuscript Section 2.4, lines 192-204)

2.4 Causal Contextual Domain Generalisation (CCDG)

Causal Contextual Domain Generalisation (CCDG) is an advanced DG approach, aiming to learn robust and transferable feature representations through exploiting causal relationships between input features, domain characteristics, and prediction targets (Ragab et al., 2022). Similar to DANN, CCDG reduces the influence of domain-specific variations on the learned representations, thereby improving generalisation to unseen domains. However, unlike conventional feature alignment approaches, CCDG introduces additional constraints to enhance the extraction of causal and domain-invariant information. In this study, CCDG is implemented as a benchmark DG method to evaluate the effectiveness of the proposed framework under varying source and target turbine conditions. CCDG enhances the class-level feature alignment by maximising the mutual information between samples belonging to the same class across different domains while minimising the mutual information between samples from different classes (Ragab et al., 2022). This enables the model to preserve discriminative features associated with scour conditions while reducing sensitivity to domain-related variations. The CCDG model is trained using a composite objective function consisting of a classification loss and a contrastive loss. The classification loss ensures accurate identification of scour states, whereas the contrastive loss promotes domain-invariant feature learning by reducing the distance between same-class samples and increasing the separation between different-class samples in the latent feature space.

A paragraph of text has been added to the revised manuscript, shown in blue text. For convenience, this is also shown below. (Relevant text from manuscript Section 4.4, lines 653-665)

The training strategy for CCDG combines supervised scour classification with a contrastive learning objective to improve the robustness of the extracted feature representations. The overall training loss consists of two complementary components: the classification loss and the contrastive loss. The classification loss is calculated using the negative log-likelihood loss and guides the model to correctly predict the scour state from the labelled source-domain samples to ensure the learned features retain the information required for accurate scour identification. The contrastive loss is applied to the latent feature representations extracted by the shared network. By using domain labels, the contrastive objective encourages samples from different domains to learn more consistent feature representations while reducing domain-specific variations. The two losses are combined to form the total training objective, where the classification loss promotes discriminative features for scour detection and the contrastive loss improves feature alignment across domains. During each iteration, the model parameters are updated by minimising this combined loss, resulting in feature representations that are both sensitive to scour-related changes and more robust against variations in turbine characteristics, environmental conditions, and operational scenarios. This approach enhances the generalisation capability of the model when applied to previously unseen turbines or offshore wind farm conditions.

A description text has been added to the revised manuscript, shown in blue text. For convenience, this is also shown below. (Relevant text from manuscript Section 4.1, lines 502)

Table 2: Training task specifications used for the model development

<table>
<tr><th>Task</th><th>Source Turbine</th><th>Target Turbine</th><th>Task Description</th></tr>
<tr><td>Task 1</td><td>{T1.1 , T2.1 , T3.1}</td><td rowspan="4">Corresponding to the remaining turbines across the three farms, including Farm 1 {T1.1- T1.11}, Farm 2 {T2.1- T2.11}, and Farm 3 {T3.1- T3.11}</td><td>Evaluation of cross-farm generalisation using shallow-water turbines with relatively low foundation stiffness as source domains.</td></tr>
<tr><td>Task 2</td><td>{T1.6 , T2.6 , T3.6}</td><td>Evaluation using intermediate water-depth and foundation stiffness conditions.</td></tr>
<tr><td>Task 3</td><td>{T1.11 , T2.11 , T3.11}</td><td>Evaluation using deep-water turbines with relatively high foundation stiffness conditions.</td></tr>
<tr><td>Task 4</td><td>{T1.1 , T2.11 , T3.6}</td><td>Evaluation using heterogeneous source turbines representing diverse foundation and environmental conditions.</td></tr>
</table>

Appendix

A paragraph of text has been added to the revised manuscript, shown in blue text. For convenience, this is also shown below. (Relevant text from manuscript Section 3.1, lines 249-255)

The foundation specifications of the OWTs at Farm 1 are provided in Appendix A (Table A1).

The detailed monopile foundation specifications for Farm 2, assumed to be founded in medium-dense sand, are presented in Appendix A (Table A2).

The monopile foundation specifications for Farm 3 are presented in Appendix A (Table A3).

A paragraph of text has been added to the revised manuscript, shown in blue text. For convenience, this is also shown below. (Relevant text from manuscript Section 3.5, lines 398-407)

The MMD distances between the healthy-state data of the reference turbines and the remaining turbines under different scour conditions are presented in Appendix A. Specifically, Table A7 reports the results for turbine T1.1 in Farm 1, Table A8 presents the corresponding results for turbine T2.1 in Farm 2, and Table A9 provides the equivalent results for turbine T3.1 in Farm 3.

The MMD distances between turbine T3.1 and the remaining turbines across all three farms under healthy conditions are presented in Appendix A (Table A10).

A paragraph of text has been added to the revised manuscript, shown in blue text. For convenience, this is also shown below. (Relevant text from manuscript Section 3.2, lines 270-271)

The environmental conditions for Farms 1–3 are presented in Appendix A (Tables A4–A6), respectively.

A paragraph of text has been added to the revised manuscript, shown in blue text. For convenience, this is also shown below. (Relevant text from manuscript Section Appendix A, lines 835)

Appendix A

Table A1: Key Specifications of OWT Foundations at Farm 1

Unit Name	Water Depth (m)	Soil Relative Density	Soil Unit Weight (kN/m^3)	Pile Diameter (m)	Wall Thickness (mm)	Embedment Depth (m)
T1.1	20.0	0.70	19.0	6	85	30
T1.2	20.5	0.72	19.1	6	85	30

T1.3	21.0	0.74	19.2	6	85	30
T1.4	21.5	0.76	19.3	6	90	30
T1.5	220	0.78	19.4	6	90	30
T1.6	22.5	0.80	19.5	6	90	30
T1.7	23.0	0.82	19.6	6	90	30
T1.8	23.5	0.84	19.7	6	95	30
T1.9	24.0	0.86	19.8	6	95	30
T1.10	24.5	0.88	19.9	6	95	30
T1.11	25.0	0.90	20.0	6	95	30

Table A2: Key Specifications of OWT Foundations at Farm 2

Unit Name	Water Depth (m)	Soil Relative Density	Soil Unit Weight (kN/m^3)	Pile Diameter (m)	Wall Thickness (mm)	Embedment Depth (m)
T2.1	20.0	0.40	18.0	6.0	90	40
T2.2	20.5	0.42	18.1	6.0	90	40
T2.3	21.0	0.44	18.2	6.0	90	40
T2.4	21.5	0.46	18.3	6.0	90	40
T2.5	220	0.48	18.4	6.0	90	40
T2.6	22.5	0.50	18.5	6.1	90	40
T2.7	23.0	0.52	18.6	6.1	90	40
T2.8	23.5	0.54	18.7	6.1	90	40
T2.9	24.0	0.56	18.8	6.1	90	40
T2.10	24.5	0.58	18.9	6.2	90	40
T2.11	25.0	0.60	19.0	6.2	90	40

Table A3: Key Specifications of OWT Foundations at Farm 3

Unit Name	Water Depth (m)	Soil Relative Density	Soil Unit Weight (kN/m^3)	Pile Diameter (m)	Wall Thickness (mm)	Embedment Depth (m)
T3.1	20.0	0.20	17.0	6.0	90	50
T3.2	20.5	0.22	17.1	6.0	90	50
T3.3	21.0	0.24	17.2	6.0	90	50
T3.4	21.5	0.26	17.3	6.0	90	50
T3.5	22.0	0.28	17.4	6.0	90	50
T3.6	22.5	0.30	17.5	6.1	90	50
T3.7	23.0	0.32	17.6	6.1	90	50
T3.8	23.5	0.34	17.7	6.1	90	50
T3.9	24.0	0.36	17.8	6.1	90	50
T3.10	24.5	0.38	17.9	6.2	90	50
T3.11	25.0	0.40	18.0	6.2	90	50

Table A4: Environmental Conditions at Farm 1

Load Case	Wind Speed (m/s)	Significant Wave Height (m)	Wave Peak Period (second)	Current Speed (m/s)
LC 1.1	10.0	1.61	5.14	0.26
LC 1.2	11.0	1.73	5.23	0.29
LC 1.3	11.5	1.79	5.28	0.30
LC 1.4	12.0	1.85	5.32	0.31
LC 1.5	12.5	1.91	5.37	0.32
LC 1.6	13.0	1.97	5.41	0.34
LC 1.7	13.5	2.03	5.46	0.35
LC 1.8	14.0	2.09	5.50	0.36
LC 1.9	14.5	2.15	5.55	0.38
LC 1.10	15.0	2.21	5.59	0.39
LC 1.11	15.5	2.27	5.64	0.40
LC 1.12	16.0	2.33	5.68	0.41

Table A5: Environmental Conditions at Farm 2

Load Case	Wind Speed (m/s)	Significant Wave Height (m)	Wave Peak Period (second)	Current Speed (m/s)
LC 2.1	9.60	1.64	5.16	0.25
LC 2.2	10.2	1.73	5.23	0.26
LC 2.3	10.8	1.81	5.30	0.28
LC 2.4	11.4	1.90	5.37	0.30
LC 2.5	12.0	1.98	5.44	0.31
LC 2.6	12.6	2.07	5.51	0.33
LC 2.7	13.2	2.15	5.58	0.34
LC 2.8	13.8	2.24	5.65	0.36
LC 2.9	14.4	2.32	5.72	0.37
LC 2.10	15.0	2.41	5.79	0.39
LC 2.11	15.6	2.49	5.86	0.40
LC 2.12	16.2	2.58	5.94	0.42

Table A6: Environmental Conditions at Farm 3

Load Case	Wind Speed (m/s)	Significant Wave Height (m)	Wave Peak Period (second)	Current Speed (m/s)
LC 3.1	9.30	1.60	5.13	0.24
LC3.2	9.90	1.69	5.20	0.26
LC 3.3	10.5	1.77	5.27	0.27
LC 3.4	11.1	1.86	5.34	0.29
LC 3.5	11.7	1.94	5.41	0.30
LC 3.6	12.3	2.03	5.48	0.32
LC 3.7	12.9	2.11	5.55	0.33

LC 3.8	13.5	2.19	5.62	0.35
LC 3.9	14.1	2.28	5.69	0.37
LC 3.10	14.7	2.36	5.76	0.38
LC 3.11	15.3	2.45	5.83	0.40
LC 3.12	15.9	2.53	5.90	0.41

Table A7: MMD value between the healthy state data of turbine T1.1 and the remaining turbines at Farm 1 under both healthy and scoured states

Scour Depth	Target Turbines										
	T 1.1	T 1.2	T 1.3	T 1.4	T 1.5	T 1.6	T 1.7	T 1.8	T 1.9	T 1.10	T 1.11
0m (Healthy)	0.00	0.02	0.12	0.20	0.32	0.28	0.36	0.44	0.48	0.52	0.52
1m	0.05	0.02	0.03	0.07	0.22	0.18	0.30	0.39	0.42	0.45	0.45
2m	0.25	0.16	0.06	0.04	0.07	0.08	0.19	0.31	0.36	0.41	0.42
3m	0.52	0.42	0.29	0.26	0.12	0.15	0.13	0.17	0.24	0.31	0.33
4m	0.72	0.64	0.55	0.53	0.36	0.37	0.24	0.21	0.20	0.25	0.27
5m	0.88	0.81	0.75	0.74	0.61	0.61	0.47	0.43	0.34	0.41	0.41
6m	1.00	0.95	0.90	0.91	0.81	0.80	0.69	0.68	0.59	0.62	0.65
7m	1.12	1.07	1.03	1.03	0.95	0.94	0.87	0.86	0.79	0.80	0.82
8m	1.21	1.17	1.15	1.16	1.08	1.06	1.00	1.00	0.94	0.95	0.98
9m	1.29	1.25	1.22	1.22	1.17	1.15	1.10	1.12	1.07	1.09	1.11

Table A8: MMD value between the healthy state data of turbine T2.1 and the remaining turbines at Farm 2 under both healthy and scoured states

Scour Depth	Target Turbines										
	T 2.1	T 2.2	T 2.3	T 2.4	T 2.5	T 2.6	T 2.7	T 2.8	T 2.9	T 2.10	T 2.11
0m (Healthy)	0.00	0.04	0.03	0.12	0.21	0.38	0.45	0.47	0.57	0.61	0.62
1m	0.03	0.01	0.01	0.05	0.12	0.28	0.36	0.38	0.50	0.55	0.56
2m	0.14	0.05	0.07	0.03	0.05	0.15	0.21	0.24	0.38	0.44	0.45
3m	0.32	0.19	0.21	0.13	0.08	0.07	0.10	0.13	0.24	0.30	0.33
4m	0.50	0.36	0.37	0.32	0.20	0.11	0.12	0.12	0.15	0.19	0.21
5m	0.64	0.52	0.53	0.51	0.36	0.26	0.27	0.27	0.17	0.19	0.20
6m	0.76	0.66	0.66	0.67	0.53	0.44	0.48	0.47	0.34	0.35	0.31
7m	0.85	0.78	0.78	0.79	0.67	0.59	0.64	0.64	0.52	0.54	0.48
8m	0.90	0.89	0.89	0.90	0.78	0.73	0.78	0.77	0.68	0.69	0.63
9m	0.90	1.00	1.01	1.01	0.90	0.84	0.89	0.88	0.80	0.81	0.77

Table A10: MMD value between the healthy state data of turbine T3.1 and the remaining turbines at Farm 3 under both healthy and scoured states

Scour Depth	Target Turbines										
	T 3.1	T 3.2	T 3.3	T 3.4	T 3.5	T 3.6	T 3.7	T 3.8	T 3.9	T 3.10	T 3.11
0m (Healthy)	0.00	0.04	0.05	0.11	0.23	0.38	0.42	0.47	0.55	0.64	0.67

1 m	0.02	0.01	0.01	0.05	0.16	0.29	0.33	0.40	0.48	0.58	0.62
2 m	0.11	0.02	0.02	0.02	0.07	0.17	0.21	0.29	0.37	0.48	0.53
3 m	0.26	0.11	0.13	0.08	0.04	0.07	0.10	0.17	0.24	0.35	0.42
4 m	0.39	0.26	0.29	0.23	0.11	0.07	0.09	0.11	0.14	0.22	0.29
5 m	0.53	0.41	0.42	0.37	0.25	0.19	0.19	0.12	0.13	0.16	0.20
6 m	0.65	0.55	0.57	0.52	0.40	0.32	0.31	0.21	0.21	0.20	0.19
7 m	0.77	0.68	0.70	0.66	0.55	0.46	0.46	0.34	0.34	0.30	0.25
8 m	0.86	0.79	0.79	0.78	0.69	0.61	0.62	0.49	0.50	0.46	0.39
9 m	0.93	0.87	0.89	0.86	0.79	0.74	0.75	0.63	0.65	0.61	0.55

Table A11: MMD distance between turbine T3.1 and the remaining turbines across different farms in the healthy state (X is 1-3 for farms 1-3)

	TX.1	TX.2	TX.3	TX.4	TX.5	TX.6	TX.7	TX.8	TX.9	TX.10	TX.11
Farm 3	0.00	0.04	0.05	0.11	0.23	0.38	0.42	0.47	0.55	0.64	0.67
Farm 2	0.71	0.73	0.73	0.80	0.82	0.90	0.96	0.96	0.98	1.02	1.00
Farm 1	1.15	1.15	1.17	1.21	1.23	1.19	1.21	1.26	1.27	1.29	1.28

References

Abdelhak, M., Prendergast, L. J., Tott-Buswell, J., Ghiasi, R., & Malekjafarian, A. (2026). Wind farm-level scour detection around offshore monopile foundations using unsupervised domain adaptation. Mechanical Systems and Signal Processing, 251, 114186. https://doi.org/https://doi.org/10.1016/j.ymssp.2026.114186

Abdelhak, M., Tott-Buswell, J., Prendergast, L. J., Ghiasi, R., & Malekjafarian, A. (2025). Scour identification around offshore wind turbine monopile foundations using an unsupervised anomaly detection approach. Ocean Engineering, 340, 122365. https://doi.org/https://doi.org/10.1016/j.oceaneng.2025.122365

Byrne, B., McAdam, R., Burd, H., Houlsby, G., Martin, C., Zdravkovic, L., Taborda, D. M. G., Potts, D., Jardine, R., Sideri, M., Schroeder, F., Gavin, K., Doherty, P., Igoe, D., Wood, A., Kallehave, D., & Gretlund, J. (2015). New design methods for large diameter piles under lateral loading for offshore wind applications. https://doi.org/10.1201/b18442-96

Cheynet, E., Jakobsen, J. B., & Obhrai, C. (2017). Spectral characteristics of surface-layer turbulence in the North Sea. Energy Procedia, 137, 414-427. https://doi.org/https://doi.org/10.1016/j.egypro.2017.10.366

Prendergast, L. J., & Gavin, K. (2016). A comparison of initial stiffness formulations for small-strain soil–pile dynamic Winkler modelling. Soil Dynamics and Earthquake Engineering, 81, 27-41. https://doi.org/https://doi.org/10.1016/j.soildyn.2015.11.006

Ragab, M., Chen, Z., Zhang, W., Eldele, E., Wu, M., Kwoh, C. K., & Li, X. (2022). Conditional Contrastive Domain Generalization for Fault Diagnosis. IEEE Transactions on Instrumentation and Measurement, 71, 1-12. https://doi.org/10.1109/TIM.2022.3154000

Tott-Buswell, J., Prendergast, L. J., & Gavin, K. (2024). A CPT-based multi-spring model for lateral monopile analysis under SLS conditions in sand. Ocean Engineering, 293, 116642. https://doi.org/https://doi.org/10.1016/j.oceaneng.2023.116642

Wolfram, J., & Naghipour, M. (1999). On the estimation of Morison force coefficients and their predictive accuracy for very rough circular cylinders. Applied Ocean Research, 21(6), 311-328. https://doi.org/https://doi.org/10.1016/S0141-1187(99)00018-8

Zefzouf, M., Chioukh, N., Castro, M., Miranda, F., Leal Sousa, R., Carvalho, E., Rosa-Santos, P., Taveira-Pinto, F., & Fazeres-Ferradosa, T. (2025). Laboratory study on scour development around a monopile in layered soils. Ocean Engineering, 342, 122968. https://doi.org/https://doi.org/10.1016/j.oceaneng.2025.122968

Zhao, D., Han, N., Goh, E., Cater, J. E., & Reinecke, A. (2019). Offshore wind turbine aerodynamics modelling and measurements. Wind Turbines and Aerodynamics Energy Harvesters.